Dynamic Pareto Optimization of Consolidated Bioprocessing for Ethanol Titer, Productivity, Conversion, and Operating Severity

Mark Korang Yeboah *, Ahmad Addo, Nana Yaw Asiedu *

Posted Date: 9 May 2026

doi: 10.20944/preprints202605.0590.v1

Keywords: consolidated bioprocessing; lignocellulosic ethanol; dynamic optimization; multi-objective optimization; Pareto optimality; optimal control; temperature and pH policies; bioprocess modeling

 doi:10.20944/preprints202605.0590.v1

Article

Dynamic Pareto Optimization of Consolidated Bioprocessing for Ethanol Titer, Productivity, Conversion, and Operating Severity

Mark Korang Yeboah [1,2,*], Ahmad Addo [2] and Nana Yaw Asiedu [2,*]

[1] Chair of Dynamics and Control, University of Duisburg–Essen, Lotharstraße, 47057 Duisburg, Germany
[2] Faculty of Mechanical and Chemical Engineering, Kwame Nkrumah University of Science and Technology, Kumasi, Ghana
* Correspondence: mark.korangyeboah@uni-due.de (M.K.Y.); nasiedusoe@yahoo.co.uk (N.Y.A.)

Abstract

Consolidated bioprocessing (CBP), where enzyme production, substrate hydrolysis, and fermentation occur in a single bioreactor, provides a promising pathway for lignocellulosic ethanol production. Nevertheless, CBP operation involves trade-offs among ethanol titer, productivity, substrate conversion, soluble sugar accumulation, batch cycle time, and the operating severity associated with temperature and pH profiles. This study introduces a feasibility-aware multi-objective dynamic optimization approach for identifying Pareto-optimal operating policies for batch CBP processes. A simplified, mechanistically driven dynamic model is developed to represent biomass growth, enzyme activity, insoluble substrate hydrolysis, soluble sugar formation and consumption, ethanol production, and inhibition under time-varying temperature and pH profiles. The multi-objective optimization simultaneously maximizes ethanol titer, productivity, and substrate conversion while minimizing sugar accumulation, operating severity, control effort, and batch time. In the main simulation run, 120,000 dynamic policies were evaluated, resulting in 5,017 feasible policies and 328 feasible Pareto-optimal policies under a minimum conversion threshold of 0.42. The optimized dynamic policy achieved an ethanol titer of 1.265 g L^{-1}, a maximum productivity of 0.017 g L^{-1} h^{-1}, and a maximum conversion of 0.440. Compared with the best static policies, the dynamic Pareto policies improved ethanol titer, productivity, and conversion by 10.6%, 8.3%, and 14.3%, respectively. The feasibility analysis showed that a conversion threshold of 0.42 is stringent but achievable, whereas thresholds of 0.44 and 0.55 were not attainable under the current dynamic model and operating range. Independent-seed repetition confirmed the existence of a consistent high-performing region across different stochastic searches. The resulting Pareto front and operating-policy charts provide a useful basis for selecting temperature and pH profiles for CBP process operation.

Keywords: consolidated bioprocessing; lignocellulosic ethanol; dynamic optimization; multi-objective optimization; Pareto optimality; optimal control; temperature and pH policies; bioprocess modeling

1. Introduction

Producing renewable liquid biofuels from lignocellulosic feedstocks has received considerable research interest over the years. Various conversion strategies have been explored; however, one particular promising approach is consolidated bioprocessing (CBP). The appeal of CBP lies in the combination of cellulase enzyme generation, cellulose hydrolysis, fermentation of hydrolyzed sugars, and end-product formation within a single biological process [1,2]. In addition, CBP may offer cost savings in terms of cellulase enzyme production relative to conventional separate hydrolysis and fermentation processes. However, the tightly coupled dynamic nature of CBP presents unique challenges to the implementation and optimization of CBP because substrate solubilization, sugar solubilization, growth, ethanol production, and inhibition effects take place concurrently during operation [3,4]. While the tight coupling makes CBP interesting, its operational complexity increases

 doi:10.20944/preprints202605.0590.v1

because various operating conditions are favorable under different process objectives. Moreover, the temperature and pH policies used to control CBP operations affect enzymatic activity and ethanol productivity. Thus, optimizing CBP requires the simultaneous consideration of multiple objectives in order to optimize the dynamic process.

Prior work in the modeling of bioprocesses has highlighted the utility of dynamic models in supporting the process design, scale-up, monitoring, and control [5]. The application of dynamic models in CBP has provided important insights into the genome-scale metabolic characteristics of *C. thermocellum* and ethanol production [6], as well as the coordination of saccharification and fermentation through mechanism-based and cybernetic analysis [7]. Data-driven studies in CBP have also shown that machine learning models can be useful in predicting yeast yield and operating conditions provided adequate experimental datasets are available [8]. More recently, studies involving literature-derived models of multi-product CBP have indicated the possibility of using endpoint-level datasets in predicting ethanol and co-product yields from CBP [9]. These studies have provided some valuable knowledge and computational insights in CBP operations, and several studies have focused on particular process objectives and operating condition policies. However, less attention has been given to the systematic construction of Pareto fronts for CBP operation. In particular, the trade-offs among ethanol titer, productivity, substrate conversion, soluble sugar accumulation, operating severity, control movement, and batch time remain insufficiently characterized.

Multi-objective optimal control provides a powerful means for analyzing and optimizing processes with conflicting objectives. The method differs from single-objective optimal control in that a set of non-dominated solutions is determined in place of finding a single solution under an assumed preference among the objectives [10]. Multi-objective optimal experiment design has also illustrated the usefulness of the technique in handling dynamic bioprocess optimization problems [11]. Evolutionary Pareto search methods provide a practical way of generating non-dominated solutions to nonlinear optimization problems [12]. On the other hand, methods such as normal boundary intersection and normalized normal constraint enable efficient generation and interpretation of the trade-off surfaces in dynamic bioprocess optimization [13,14]. Given that objectives are likely to be in conflict in many biological processes, Pareto methods are highly useful for studying the dynamic behaviors and potential optimization of bioprocesses.

The current study investigates the Pareto optimization of the CBP operation problem through the construction of feasible Pareto fronts and operating policies. The manipulated variables for CBP include time-varying temperature and pH profiles along with the terminal batch time. The state variables for CBP consist of biomass, cellulase activity, insoluble substrate, soluble sugars, ethanol concentration, and inhibition effects. The process objectives involve maximizing ethanol titer, productivity, and conversion while minimizing soluble sugar, temperature and pH severities, control movements, and batch time. Specifically, CBP operations are investigated using a feasible Pareto optimization method with a view to selecting suitable policies under different process objectives.

The principal contribution of the study lies in developing a Pareto optimization method for mapping the operating policies of CBP operation problems. As opposed to data-driven or trial-and-error approaches, the study employs dynamic optimization for CBP operations and generates the Pareto fronts and operating policies. Based on the Pareto fronts and tradeoff surfaces, it is possible to identify the dynamic policy space in which ethanol productivity, substrate conversion, mildness, and controllability are compatible and when severe trade-offs are inevitable. This provides a theoretical basis for selecting optimal operating policies under different process objectives for CBP operations.

The rest of this paper is organized as follows. Section 2 introduces the dynamic CBP model and the state, control, and kinetic equations. Section 3 formulates the multi-objective dynamic optimization of CBP operation problems, including objective functions, feasibility constraints, control policies, and Pareto generation. Section 4 analyzes the Pareto fronts and dynamic operating policies obtained, including representative dynamic processes, Pareto policy maps, and feasibility sensitivity and repeatability. Section 5 concludes the study.

 doi:10.20944/preprints202605.0590.v1

2. Dynamic Model of CBP

A reduced-order dynamic model was employed for representing the batch CBP with time-varying temperature and pH conditions. Such a dynamic CBP model does not attempt to resolve the entire metabolic network in the microorganism or the distributed structure of the cellulose particles. Rather, it provides an approximate grey-box representation of the key mechanisms of CBP necessary for multi-objective optimization: microbial growth, enzyme formation, cellulose degradation to soluble sugar, sugar accumulation due to hydrolysis-faster-than-fermentation conditions, sugar consumption for ethanol production, and ethanol inhibition effects. Such compact representations are commonly used for bioprocess optimization and scale-up [5,10]. On the other hand, the model retains the key features distinguishing CBP from separate hydrolysis and fermentation approaches to microbial cellulose utilization [1,2]. While more detailed CBP models, including the coordinated enzymatic and genome-scale models, provide additional insights into biological processes, they are more computationally expensive for optimization tasks [6,7,15].

2.1. Process Description

The modeled process involves a batch CBP in a well-mixed reactor in which the microorganism converts an insoluble lignocellulosic substrate to ethanol via multiple biological and biochemical steps. First, microbial cells are grown in the presence of the insoluble substrate, producing the hydrolytic enzymes; second, the enzymes promote the conversion of the insoluble substrate to the soluble sugar, which in turn is used up by the cells for further ethanol production. The sequence of reactions resembles the overall concept of CBP developed for microbial cellulose utilization [1]. More recent efforts focused on developing a coordinated enzymatic control strategy for cellulolytic systems such as *Clostridium thermocellum* [3].

Hydrolysis and fermentation occurring in parallel are essential in this model. If the reaction rate of hydrolysis exceeds the one of fermentation, the soluble sugar pool will accumulate; similarly, excessive fermentation demands result in lower hydrolysis rates. Both temperature and pH values have an impact on the kinetics, yet the ideal conditions for each of these rates can be different, thus leading to an inherent operational conflict. Coordinated enzymatic modeling of *C. thermocellum* has indicated that cellulose solubilization and ethanol fermentation are tightly coupled phenomena in CBP [7]. Moreover, kinetic analysis of the fermentation of *C. thermocellum* has pointed out the significant role of growth, inhibition, and substrate-dependent kinetics [16].

While the current model is relatively compact, genome-scale and core kinetic metabolic models can provide more insights into intracellular metabolic processes [6,17]. Also, cybernetic and population balance descriptions may provide further details on the enzyme distribution in the environment or the heterogeneous structure of the cellulose particles [7]. However, such level of detail is not important here, since the goal is to generate a simplified dynamic model for large-scale simulation and policy archive evaluation. Thus, it should be easy enough to simulate and provide sufficient information about the main process couplings.

2.2. States and Manipulated Variables

The dynamic state vector in the problem can be represented as

$$x(t) = \begin{bmatrix} X(t) & E(t) & B(t) & C(t) & P(t) \end{bmatrix}^{\top}, \tag{1}$$

where X is the biomass concentration, E is the total enzyme activity, B is the insoluble substrate pool, C is the soluble sugar pool, and P is the ethanol concentration. The use of biomass, substrate, sugar, and product pools follows typical bioreactor dynamic representations reported in the literature [5,16]. The state variables and manipulated variables considered in the model are summarized in Table 1.

 doi:10.20944/preprints202605.0590.v1

The manipulated variable vector is

$$u(t) = \begin{bmatrix} T(t) & \mathrm{pH}(t) \end{bmatrix}^{\top}, \tag{2}$$

where $T(t)$ is the reactor temperature and $\mathrm{pH}(t)$ is the reactor pH value. In addition to temperature and pH, the batch final time, t_f, is considered an optimization decision. The manipulated variables were selected because of their strong influence on cellulase activity, microbial growth, and fermentation in lignocellulosic bioprocessing [3,7]. Temperature and pH were restricted to the ranges

$$30 \leq T(t) \leq 55, \qquad 5.0 \leq \mathrm{pH}(t) \leq 8.0. \tag{3}$$

Table 1. Dynamic model states and manipulated variables.

Symbol	Description	Role
$X(t)$	Biomass concentration	State
$E(t)$	Total enzyme activity	State
$B(t)$	Insoluble substrate pool	State
$C(t)$	Soluble sugar pool	State
$P(t)$	Ethanol concentration	State
$T(t)$	Reactor temperature	Manipulated variable
$\mathrm{pH}(t)$	Reactor pH	Manipulated variable
t_f	Final batch time	Decision variable

2.3. Phase-Weighted Kinetic Structure

The dynamical model of CBP takes the form

$$\frac{dx(t)}{dt} = f(x(t), u(t), \theta), \qquad x(0) = x_0, \tag{4}$$

where θ is the kinetic parameter set. Phase-weighted functions are used to describe the transition through phases of growth, hydrolysis, and fermentation:

$$\omega_1(t) = \frac{1}{1 + \exp[k(t - t_1)]}, \tag{5}$$

$$\omega_3(t) = \frac{1}{1 + \exp[-k(t - t_2)]}, \tag{6}$$

$$\omega_2(t) = \max(0, 1 - \omega_1(t) - \omega_3(t)), \tag{7}$$

where ω_1, ω_2, and ω_3 correspond to the growth/enzyme-formation, hydrolysis, and fermentation phases, respectively. Parameters t_1, t_2, and k determine the timing and smoothness of the phase transitions. In the simulations, the parameter values were $t_1 = 18$ h, $t_2 = 44$ h, and $k = 0.28$. Phase weighting allows the batch progression through biologically meaningful stages to be represented without discontinuous switching. This approach approximates biological phase transitions in a computationally tractable manner.

Growth and enzyme activities are described by

$$\frac{dX}{dt} = \omega_1(t)\left[(\mu(T, \mathrm{pH}, P) - k_d(P))X\left(1 - \frac{X}{K_X}\right)\right], \tag{8}$$

$$\frac{dE}{dt} = \omega_1(t)[Y_E(T, \mathrm{pH})X - k_E(T)E], \tag{9}$$

where μ is the growth rate depending on temperature, pH, and ethanol concentration, k_d is the ethanol-associated enzyme deactivation coefficient, K_X is the biomass carrying capacity, Y_E is the enzyme formation yield, and k_E is the enzyme deactivation rate. Such a simple Monod-type growth kinetics, including the inhibition effect on the growth, is common in batch fermentation models [16]. In cases

 doi:10.20944/preprints202605.0590.v1

where a model is used for optimization rather than metabolic network exploration, it is preferable to use compact reduced-order growth kinetics.

Hydrolysis of the substrate to the soluble sugar is determined as follows:

$$v_h(t) = V_h(T, \mathrm{pH}, S_0)\frac{B(t)}{K_h + B(t)}\tanh(E(t)), \tag{10}$$

$$\frac{dB}{dt} = -\omega_2(t)v_h(t), \tag{11}$$

where the term $\frac{B}{K_h+B}$ describes the non-linear dependence on the amount of accessible insoluble substrate, V_h is the maximum hydrolysis rate depending on temperature, pH, and substrate loading, and the term tanh takes into account enzyme-mediated catalysis of the reaction, which depends on the amount of enzymes. Such a kinetics, while compact, resembles the more detailed descriptions in which adsorption onto cellulose particles and cellulose accessibility are taken into consideration [7].

Soluble sugar balance in the batch can be described as

$$\frac{dC}{dt} = \omega_2(t)[v_h(t) - k_C C(t)] - \omega_3(t)v_p(t), \tag{12}$$

where k_C is the sugar consumption rate coefficient occurring during the hydrolysis-dominant phase. Sugar production and consumption are critical for CBP in order to establish its difference from isolated hydrolysis and fermentation, thus making the above balance key to the model.

Production of ethanol in the reactor is assumed to occur in accordance with the following relations:

$$v_p(t) = Y_P(T, \mathrm{pH})\frac{C(t)}{1 + k_I(T, \mathrm{pH})P(t)}, \tag{13}$$

$$\frac{dP}{dt} = \omega_3(t)v_p(t), \tag{14}$$

where Y_P is the ethanol production coefficient and k_I is the ethanol inhibition coefficient. The denominator accounts for the reduction in the effective fermentation rate as ethanol accumulates, consistent with inhibition terms used in fermentation kinetics and CBP modeling studies [16,17].

2.4. Temperature and pH Dependent Activity Functions

The effect of temperature and pH is captured by activity functions associated with growth, hydrolysis, and fermentation. It is necessary to include distinct temperature and pH functions since the optimal operating regime for enzymatic activity, microbial growth, and ethanol formation may differ. Such temperature–pH conflicts were reported in integrated HFFS schemes, whereby favorable conditions for enzymatic saccharification are not necessarily ideal for microbial ethanol production [18]. A similar problem arises in CBP operations where enzyme production, substrate hydrolysis, and fermentation all take place in the same reactor [3,7].

For each kinetic process ($z = g, h, f$, denoting growth, hydrolysis, and fermentation, respectively), a temperature activity function is expressed by

$$\phi_z(T) = \mathrm{clip}\left[\exp\left(-\left(\frac{T - T_z^*}{\sigma_{T,z}}\right)^2\right), \phi_{\min}, \phi_{\max}\right], \tag{15}$$

and a pH activity function is expressed by

$$\psi_z(\mathrm{pH}) = \mathrm{clip}\left[\exp\left(-\left(\frac{\mathrm{pH} - \mathrm{pH}_z^*}{\sigma_{\mathrm{pH},z}}\right)^2\right), \psi_{\min}, \psi_{\max}\right], \tag{16}$$

where T_z^* and pH_z^* denote the nominal centers of the activity distributions, while $\sigma_{T,z}$ and $\sigma_{\mathrm{pH},z}$ control their widths. Clipping ensures numerical stability of the solution procedure since overly large or zero

 doi:10.20944/preprints202605.0590.v1

correction factors may arise in policy search. The growth, hydrolysis, and fermentation rate coefficients are then written as

$$\mu(T, \mathrm{pH}, P) = \mu_{\max}\phi_g(T)\psi_g(\mathrm{pH}), \tag{17}$$

$$Y_E(T, \mathrm{pH}) = Y_{E,\max}\phi_g(T)\psi_g(\mathrm{pH})\chi_{\mathrm{pret}}, \tag{18}$$

$$V_h(T, \mathrm{pH}, S_0) = V_{h,\max}\phi_h(T)\psi_h(\mathrm{pH})\chi_{\mathrm{pret}}\chi_S, \tag{19}$$

$$Y_P(T, \mathrm{pH}) = Y_{P,\max}\phi_f(T)\psi_f(\mathrm{pH}), \tag{20}$$

where χ_{pret} and χ_S are pretreatment and substrate-loading dependent correction factors. For the simulations, the nominal centers of the temperature and pH curves were approximately 48 °C and pH 5.6 for growth, 50 °C and pH 5.2 for hydrolysis, and 42 °C and pH 6.0 for fermentation. The separation between optima creates a reason for superior performance of dynamic policies compared to constant temperature and pH schedules in CBP operation. Since all three kinetic processes cannot be optimized simultaneously under constant conditions, dynamic operation allows to emphasize some processes more than others at different stages of the batch cycle [10,18].

2.5. Severity and Feasibility Quantities

The concept of severity is not incorporated into the state variables explicitly. Instead, the instantaneous severity function is derived from the temperature and pH dynamics and serves as an optimization objective. By using the severity as a goal variable, the optimizer can differentiate policies producing similar amounts of ethanol or conversions under different severities. The severity penalty function depends on the temperature and pH deviations from reference values that correspond to mild operating regimes:

$$s_{\mathrm{sev}}(t) = \left(\frac{T(t) - T_{\mathrm{ref}}}{\Delta T}\right)^2 + \left(\frac{\mathrm{pH}(t) - \mathrm{pH}_{\mathrm{ref}}}{\Delta \mathrm{pH}}\right)^2. \tag{21}$$

Then, the severity objective is defined as the time average of the corresponding instantaneous penalties:

$$J_{\mathrm{sev}} = \frac{1}{t_f}\int_0^{t_f} s_{\mathrm{sev}}(t)\, dt. \tag{22}$$

Normalizing the severity makes it comparable across policies with different batch durations. The averaging procedure is a well-established way to quantify severity in biochemical operations [15]. Penalizing extreme temperature and pH conditions is appropriate for CBP because such conditions may enhance selected kinetic processes while also increasing control complexity or reducing biological tolerance [3].

Control effort is defined in terms of the control changes of the piecewise-constant temperature and pH trajectories:

$$J_{\Delta u} = \sum_{j=1}^{N_u - 1}\left[\left(T_{j+1} - T_j\right)^2 + \left(\mathrm{pH}_{j+1} - \mathrm{pH}_j\right)^2\right]. \tag{23}$$

Minimizing control effort is a common approach to improving operational feasibility while retaining the benefits of time-varying policies [5,10].

Conversion is calculated by comparing the insoluble substrate pool size at the start and at the end of the batch:

$$X_{\mathrm{conv}} = \frac{B(0) - B(t_f)}{B(0)}. \tag{24}$$

A policy is said to be feasible if it meets the conversion threshold and the soft sugar constraint:

$$X_{\mathrm{conv}} \geq X_{\mathrm{conv,min}}, \qquad C(t) \leq C_{\max}. \tag{25}$$

 doi:10.20944/preprints202605.0590.v1

The conversion threshold used in the main study was set to $X_{conv,min} = 0.42$ and the sugar concentration threshold was set to $C_{max} = 6$ g L^{-1}. Conversion threshold was further analyzed in the sensitivity study to avoid the use of one particular model-dependent value. A threshold for sugar accumulation was included because high sugar concentration implies an imbalance between hydrolysis and fermentation, which is a fundamental problem in HFFS CBP [7].

2.6. Model Assumptions

The model includes several assumptions, some of which limit model fidelity while others affect its computational efficiency. First, the reactor is assumed to be perfectly mixed, hence the concentration of biomass, enzyme, insoluble substrate, soluble sugar, ethanol, temperature, and pH are homogeneous throughout the volume. Perfect mixing is a reasonable assumption for a reduced-order policy-screening model, however, this assumption will need to be revised if scaling up to a larger reactor is required [5]. Second, insoluble substrate and soluble sugar are represented by lumped pools that ignore cellulose and hemicellulose breakdown and subsequent monomerization into sugars. Lumping reduces computational cost while keeping the key aspect of hydrolysis-fermentation coupling.

Third, enzyme activity is represented by a single lumped activity factor and enzyme composition is not modeled explicitly. Cellulases kinetics and coordinated control models allow for a detailed description of enzymatic action, including the allocation of cellulase components [7]. Fourth, ethanol is the only explicitly mentioned fermentation product. Other compounds such as acetate, lactate, hydrogen, carbon dioxide, and organic acids are lumped into the yield and inhibition expressions. This is reasonable in the context of an ethanol-oriented dynamic optimization study, but other studies have shown that co-product formation plays an increasingly important role when broader biorefinery goals are addressed [9].

Fifth, temperature and pH are assumed to be directly controllable variables with bounds and implemented as piecewise-constant control sequences. Finally, the current formulation assumes a deterministic system; uncertainties in parameter values, process noise, contamination risks, and feedstock composition are not accounted for in this formulation. Robust or uncertainty-aware formulations would have to be developed prior to experimental validation, due to potentially significant variability of kinetic parameters and feedstocks in CBP processes [19,20].

Such assumptions make the model appropriate for fast-throughput dynamic optimization and Pareto front computation. Moreover, this set of assumptions defines the scope of the results interpretation, which is that the calculated policies reflect optimal strategies according to the proposed model and show the trade-offs between CBP objectives, and not experimentally determined kinetic optima. Several approaches, such as genome scale models, kinetic metabolic models, cybernetic models, and population balance equations of cellulose depolymerization, offer good comparison benchmarks for possible model extensions in the future [6,7,17]. Nevertheless, these models would be computationally expensive to apply in this type of analysis.

3. Formulation of Multi-Objective Dynamic Optimization Problem

The dynamic CBP model described in Section 2 represents a nonlinear batch process with the operating policy being the temperature and pH profile over time. The task of optimization is not to find some globally optimal policy, but to generate a set of policies with different characteristics that highlight the trade-off between ethanol titer, productivity, substrate conversion, sugar accumulation, severity of operation, control moves, and batch time. It has been observed that multi-objective optimal control is effective in analyzing dynamic bioprocesses as it can uncover operating alternatives that cannot be found by collapsing several competing objectives into a single scalarized one [10]. Similar results have been obtained in optimal experimental design where dynamic biological systems often need to balance several conflicting criteria [11]. Here, a non-dominated sorting algorithm is applied to preserve non-dominated policies based on the Pareto-ranking concept common to evolutionary multi-objective optimization algorithms [12]. Other scalarizing approaches such as normal boundary intersection and normalized normal constraint method can serve as benchmarks for finding Pareto

 doi:10.20944/preprints202605.0590.v1

fronts [13,14]; however, a direct policy search formulation is used in this paper since it allows us to efficiently explore a large archive of non-linear dynamic CBP policies without solving separate nonlinear programming problems for each preference vector.

3.1. Optimal Control Problem

Consider the dynamic state vector as

$$x(t) = \begin{bmatrix} X(t) & E(t) & B(t) & C(t) & P(t) \end{bmatrix}^\top, \tag{26}$$

where X is biomass, E is enzyme activity, B is insoluble substrate, C is soluble sugar, and P is ethanol concentration. Temperature and pH are the manipulated inputs:

$$u(t) = \begin{bmatrix} T(t) & \mathrm{pH}(t) \end{bmatrix}^\top. \tag{27}$$

The batch final time t_f is optimized as well since the best batch duration depends on the product and process characteristics [21,22]. The general multi-objective dynamic optimization problem takes the form:

$$\min_{u(t),t_f} \mathbf{J}(u, t_f) = \begin{bmatrix} J_{\mathrm{EtOH}}, J_{\mathrm{prod}}, J_{\mathrm{conv}}, J_{\mathrm{sugar}}, J_{\mathrm{sev}}, J_{\Delta u}, J_{\mathrm{time}} \end{bmatrix}, \tag{28}$$

subject to the dynamic CBP model:

$$\dot{x}(t) = f(x(t), u(t), \theta), \qquad 0 \le t \le t_f, \tag{29}$$

$$x(0) = x_0, \tag{30}$$

and operating constraints:

$$T_{\min} \le T(t) \le T_{\max}, \tag{31}$$

$$\mathrm{pH}_{\min} \le \mathrm{pH}(t) \le \mathrm{pH}_{\max}, \tag{32}$$

$$t_{f,\min} \le t_f \le t_{f,\max}. \tag{33}$$

In the main simulation, temperature and pH are confined to the ranges

$$30 \le T(t) \le 55, \qquad 5.0 \le \mathrm{pH}(t) \le 8.0, \qquad 36 \le t_f \le 144\ \mathrm{h}. \tag{34}$$

Feasibility conditions are enforced via dynamic simulation of the system. A policy is deemed feasible if it satisfies both substrate conversion and sugar accumulation requirements:

$$X_{\mathrm{conv}} \ge X_{\mathrm{conv,min}}, \tag{35}$$

$$C(t) \le C_{\max}. \tag{36}$$

The feasibility criterion in the main experiments is $X_{\mathrm{conv,min}} = 0.42$, while the soft constraint for sugar concentration is $C_{\max} = 6\ \mathrm{g\ L^{-1}}$. The substrate conversion threshold is further analyzed using sensitivity analysis, since feasible conversion is model-specific and depends on kinetic parameters and operational bounds.

3.2. Policy Parameterization

The temperature and pH profiles are parameterized using piecewise constant dynamic policies over N_u control intervals. In the main experiment, $N_u = 16$. Given the batch final time t_f, the policy grid becomes:

$$0 = \tau_0 < \tau_1 < \cdots < \tau_{N_u} = t_f, \tag{37}$$

 doi:10.20944/preprints202605.0590.v1

and the control strategy is defined as

$$u(t) = \begin{bmatrix} T_j & \mathrm{pH}_j \end{bmatrix}^\top, \qquad \tau_{j-1} \le t < \tau_j, \qquad j = 1, \ldots, N_u. \tag{38}$$

In this way, each policy candidate is described by

$$\pi = \left[T_1, \ldots, T_{N_u}, \mathrm{pH}_1, \ldots, \mathrm{pH}_{N_u}, t_f \right]. \tag{39}$$

Through the direct parameterization, the dynamic optimization problem is transformed into a policy search problem in a finite dimensional space. This kind of parameterization is very common in dynamic optimization since it allows the use of nonlinear operating strategies in an interpretable and computationally tractable form while still preserving the time dependence of the control variables [10]. In this study, the same formulation also supports high-throughput evaluation of feasible and infeasible CBP policies, which is useful for constructing a clear Pareto archive.

3.3. Performance Objectives

The performance objectives are computed based on the results of the dynamic simulation from $t = 0$ to $t = t_f$. As the problem formulation in Eq. (28) implies a minimization problem setup, naturally maximized objectives are scaled by the factor of -1.

3.3.1. Final Ethanol Titer

The ethanol-titer objective maximizes the terminal concentration of the ethanol product:

$$J_{\mathrm{EtOH}} = -P(t_f). \tag{40}$$

The ethanol titer represents the traditional batch termination criterion and is included as a benchmark measure to evaluate the performance of alternative high-titer policies.

3.3.2. Volumetric Productivity

The volumetric productivity objective maximizes the ethanol production rate per unit of batch duration:

$$J_{\mathrm{prod}} = -\frac{P(t_f) - P(0)}{t_f}. \tag{41}$$

Because $P(0) = 0$, the function simplifies to $-P(t_f)/t_f$. The productivity objective is included to prevent the selection of a high-end ethanol titer at the cost of excessively long batch duration.

3.3.3. Substrate Conversion

The conversion objective maximizes the proportion of the consumed insoluble substrate:

$$J_{\mathrm{conv}} = -X_{\mathrm{conv}} = -\frac{B(0) - B(t_f)}{B(0)}. \tag{42}$$

The inclusion of the substrate conversion objective prevents the optimization from favoring inefficient policies in terms of the utilization of the available substrates.

3.3.4. Sugar Accumulation

Soluble sugars accumulation is minimized by maximizing the time-average of their concentration:

$$J_{\mathrm{sugar}} = \frac{1}{t_f} \int_0^{t_f} C(t)\, dt. \tag{43}$$

 doi:10.20944/preprints202605.0590.v1

In this objective, a policy generating faster release of soluble sugars compared to the speed of consumption during the fermentation stage is penalized. Sugar accumulation serves as a convenient metric of the imbalance in CBP between the hydrolysis and fermentation stages.

3.3.5. Operating Severity

The thermal and pH severity are minimized compared to mild conditions:

$$J_{\text{sev}} = \frac{1}{t_f}\int_0^{t_f}\left[\left(\frac{T(t)-T_{\text{ref}}}{\Delta T}\right)^2+\left(\frac{\text{pH}(t)-\text{pH}_{\text{ref}}}{\Delta \text{pH}}\right)^2\right]dt. \tag{44}$$

T_{ref} and pH_{ref} are defined as the values representing mild conditions near the preferred region of the nominal CBP process dynamics. Operating severity is included as an objective in order to distinguish between high-performance operating policies requiring aggressive conditions and those providing acceptable results under milder settings.

3.3.6. Control Movement

Aggressive temperature and pH adjustments are discouraged by minimizing the control movement objective:

$$J_{\Delta u} = \sum_{j=1}^{N_u-1}\left[\left(T_{j+1}-T_j\right)^2+\left(\text{pH}_{j+1}-\text{pH}_j\right)^2\right]. \tag{45}$$

This penalty favors the smoother execution of the policies for CBP and thus facilitates the implementation of the resulting solution.

3.3.7. Batch Duration

Finally, the batch-time objective is included to minimize the batch duration:

$$J_{\text{time}} = t_f. \tag{46}$$

The inclusion of t_f as an objective variable allows the identification of both shorter and longer optimal batches depending on whether productivity or substrate conversion dominates the optimization problem setup, respectively. Residence time is known as a major source of the conflict between the productivity and conversion objectives.

The seven objective functions used for the Pareto optimality analysis together with the direction of their optimization and physical interpretation are listed in Table 2.

Table 2. Objective functions for the dynamic Pareto optimization problem.

Objective	Mathematical form	Direction	Interpretation
Ethanol titer	$P(t_f)$	Maximize	Final ethanol concentration
Productivity	$\left[P(t_f)-P(0)\right]/t_f$	Maximize	Volumetric ethanol productivity
Conversion	$\left[B(0)-B(t_f)\right]/B(0)$	Maximize	Fraction of insoluble substrate consumed
Sugar accumulation	$t_f^{-1}\int_0^{t_f} C(t)\,dt$	Minimize	Average soluble sugar buildup
Severity	$t_f^{-1}\int_0^{t_f} s_{\text{sev}}(t)\,dt$	Minimize	Temperature and pH operating severity
Control movement	$\sum_{j=1}^{N_u-1}\left[(\Delta T_j)^2+(\Delta \text{pH}_j)^2\right]$	Minimize	Smoothness of the operating policy
Batch time	t_f	Minimize	Duration of the batch

3.4. Pareto Optimality and Domination

A dynamic policy π_a is considered to dominate another dynamic policy π_b when it is no worse in any objective and strictly better in at least one objective. Using the minimization vector $\mathbf{J}$, the dominance relation is expressed as

$$\pi_a \prec \pi_b \iff J_i(\pi_a) \le J_i(\pi_b)\ \forall i \quad \text{and} \quad J_k(\pi_a) < J_k(\pi_b) \text{ for at least one } k. \tag{47}$$

 doi:10.20944/preprints202605.0590.v1

If there is no other feasible policy that dominates a given policy, then that policy is considered Pareto optimal. The collection of non-dominated feasible policies forms the Pareto set, while their corresponding objective values form the Pareto front. This concept is useful for analyzing CBP operation because a single scalar criterion can obscure important process trade-offs. For example, maximizing ethanol titer may require a longer batch time, whereas maximizing productivity may favor earlier termination with a lower final ethanol concentration. Similar trade-offs have motivated Pareto-based formulations in fed-batch bioreactor optimization and dynamic bioprocess optimal control [10,23].

3.5. Feasibility-Aware Pareto-Front Generation

The computational procedure is feasibility-aware. Dynamic policies are first simulated using the CBP dynamic model. Ethanol titer, productivity, conversion, sugar accumulation, operating severity, control movement, and batch time are then calculated from the simulated trajectories. Policies that satisfy the conversion and sugar constraints are classified as feasible. Non-dominated sorting is then applied preferentially to the feasible archive, using the same basic dominance logic commonly used in evolutionary Pareto optimization algorithms [12]. When feasible policies are available, the Pareto analysis is performed only on the feasible subset. This ensures that the reported Pareto set represents implementable operating strategies rather than high-performing but infeasible policies.

The algorithm begins by generating an initial archive of random dynamic policies over the admissible temperature, pH, and batch-time bounds. Each policy is then simulated and evaluated. Feasible non-dominated policies are identified and used to guide the generation of new candidate policies. These offspring policies are produced by perturbing and recombining high-performing archive members. The process is repeated for a prescribed number of generations. The final archive contains all evaluated policies, while the main Pareto set is extracted from the feasible subset. This archive-based approach is especially useful for nonlinear dynamic optimization because it preserves both feasible and infeasible policy information, allowing later analysis of feasibility limits and sensitivity thresholds.

The feasibility-aware policy-search procedure is summarized in Table 3.

Table 3. Feasibility-aware dynamic Pareto policy-search procedure.

Step	Procedure
1	Generate an initial population of dynamic temperature, pH, and batch-time policies.
2	Simulate each policy using the dynamic CBP model from $t = 0$ to $t = t_f$.
3	Compute ethanol titer, productivity, conversion, sugar accumulation, severity, control movement, and batch time.
4	Mark policies as feasible if they satisfy the conversion and sugar constraints.
5	Apply non-dominated sorting to the feasible policy archive.
6	Generate offspring policies by perturbing and recombining high-performing archive members.
7	Repeat simulation, feasibility screening, and Pareto sorting for all generations.
8	Select representative Pareto policies for maximum ethanol, maximum productivity, maximum conversion, minimum sugar, minimum severity, minimum batch time, and balanced-knee operation.

This technique is conceptually related to NSGA-II-style non-dominated sorting [12]. However, the implementation used here is a direct dynamic policy-search archive tailored to the CBP model rather than a standard evolutionary Pareto algorithm. Scalarization methods, such as weighted sums, are simple and widely used, but they can miss nonconvex regions of a Pareto front. Normal boundary intersection provides a structured way to sample trade-off surfaces [13], while the normalized normal constraint method was developed to improve Pareto-front representation in multi-objective design problems [14]. In dynamic bioprocess optimization, direct optimal-control and Pareto-generation toolkits have also been used to construct trade-off sets for nonlinear systems [10]. The archive-based

 doi:10.20944/preprints202605.0590.v1

approach used here is appropriate because the CBP problem includes nonlinear dynamics, free terminal time, feasibility thresholds, and objective functions with different physical units.

3.6. Representative Policy Selection

Once the feasible Pareto set is obtained, representative policies are selected to make the trade-offs easier to interpret. Six extreme Pareto policies are chosen by optimizing one objective at a time within the feasible Pareto set:

$$\pi_{\mathrm{EtOH}} = \arg\max_{\pi\in\mathcal{P}} P(t_f), \tag{48}$$

$$\pi_{\mathrm{prod}} = \arg\max_{\pi\in\mathcal{P}} \frac{P(t_f) - P(0)}{t_f}, \tag{49}$$

$$\pi_{\mathrm{conv}} = \arg\max_{\pi\in\mathcal{P}} X_{\mathrm{conv}}, \tag{50}$$

$$\pi_{\mathrm{sugar}} = \arg\min_{\pi\in\mathcal{P}} J_{\mathrm{sugar}}, \tag{51}$$

$$\pi_{\mathrm{sev}} = \arg\min_{\pi\in\mathcal{P}} J_{\mathrm{sev}}, \tag{52}$$

$$\pi_{\mathrm{time}} = \arg\min_{\pi\in\mathcal{P}} t_f, \tag{53}$$

where $\mathcal{P}$ is the feasible Pareto set. These extreme policies are not necessarily recommended operating points. Rather, they are used to reveal the performance limits associated with each individual process priority.

A balanced-knee Pareto policy is also selected as a practical compromise when no single objective is intended to dominate the decision. Before selecting this policy, the objectives are normalized so that larger values indicate better performance. The policy whose normalized objective vector is closest to the ideal normalized point is then chosen:

$$\pi_{\mathrm{knee}} = \arg\min_{\pi\in\mathcal{P}} \|\mathbf{z}^* - \mathbf{z}(\pi)\|_2, \tag{54}$$

where $\mathbf{z}^*$ is the ideal normalized objective vector and $\mathbf{z}(\pi)$ is the normalized performance vector of policy π. This balanced-knee selection provides a useful compromise solution when the decision requires simultaneous consideration of titer, productivity, conversion, severity, smoothness, sugar accumulation, and batch duration.

3.7. Baseline, Sensitivity, and Repeatability Analyses

Three additional analyses are included to support interpretation of the Pareto results. First, static baseline policies are evaluated using constant temperature, constant pH, and fixed batch times. This baseline is used to determine whether dynamic operation provides a meaningful advantage over constant-operation schedules. Such comparisons are important because dynamic control policies should be evaluated against simpler alternatives before being proposed as process-design tools.

Second, the minimum acceptable conversion threshold is varied to examine how strongly the feasible region depends on the chosen feasibility definition. This sensitivity analysis is important because feasibility thresholds in model-based bioprocess optimization depend partly on the assumed kinetic parameters, operating bounds, and substrate representation.

Third, independent-seed repeatability runs are performed to check whether the main performance envelope is an artifact of a single random initialization. Stochastic multi-objective searches can produce different numbers of feasible and non-dominated policies across seeds, even when the best attainable performance region remains similar. The repeatability analysis therefore evaluates whether the main conclusions are robust to stochastic search variation.

 doi:10.20944/preprints202605.0590.v1

3.8. Numerical Implementation and Computational Reproducibility

For high-throughput evaluation, the dynamic model was integrated using fixed-step numerical simulation. In the main run, the archive contained 120,000 evaluated policies, consisting of 16,000 initial policies and 14 generations with 10,000 offspring policies per generation. Each candidate policy was described by 16 temperature segments, 16 pH segments, and one terminal-time decision. GPU acceleration was used when available to speed up large candidate-scoring operations. Data handling, plotting, Pareto sorting, static-baseline analysis, feasibility-threshold sensitivity, and independent-seed repeatability summaries were performed on the CPU.

To support computational reproducibility, the workflow was implemented in Python 3.13.5 and developed in Visual Studio Code. The main stochastic Pareto search used a fixed random seed of 42, while the repeatability analysis used independent additional seeds. The computational workflow used NumPy 2.3.2 for vectorized numerical operations, pandas 2.3.1 for tabular data handling, Matplotlib 3.10.3 for figure generation, and OpenPyXL-supported Excel export. Optional GPU acceleration was provided through CuPy, with Torch used only to expose CUDA library paths on compatible Windows installations.

The full computational workflow, from dynamic CBP modeling and policy generation to feasibility-aware Pareto analysis and post-optimization interpretation, is summarized in Figure 1.

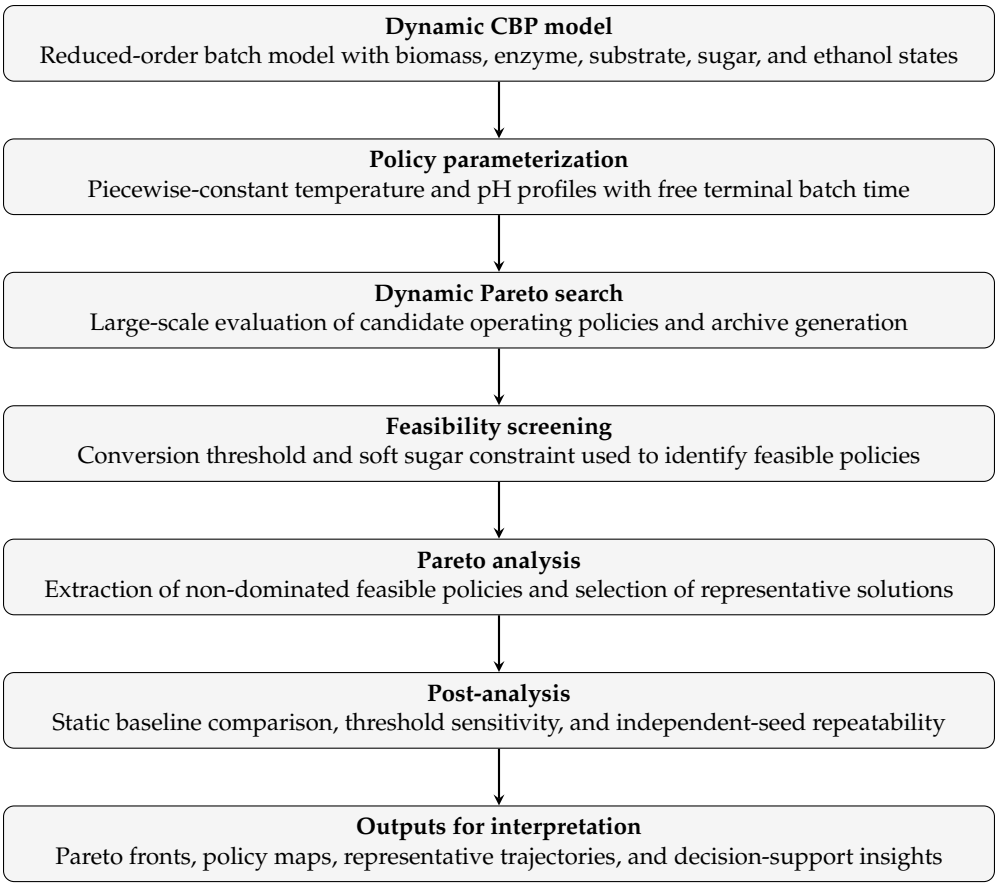

Figure 1. Workflow of the feasibility-aware multi-objective dynamic optimization framework for consolidated bioprocessing.

4. Results and Discussion

4.1. Optimization Scale, Feasibility, and Static Baseline Comparison

The dynamic Pareto optimization explored 120,000 candidate operating policies over the batch horizon. Under the main feasibility definition, which imposed a minimum substrate conversion of 0.42, 5,017 policies were classified as feasible and 328 policies were retained in the main non-dominated Pareto set. This feasible Pareto set spanned a wide range of operating priorities, including high ethanol

 doi:10.20944/preprints202605.0590.v1

titer, high productivity, high substrate conversion, low sugar accumulation, low operating severity, low control movement, and short batch duration. Within the feasible Pareto archive, the highest ethanol titer was 1.265 g L^{-1} and the maximum substrate conversion reached 0.440. Among the retained Pareto policies, the lowest severity value was 0.027, while the shortest feasible batch time was 51.46 h.

To assess the benefit of dynamic operation, a static baseline grid was evaluated using constant temperature, constant pH, and different batch termination times. For each performance criterion, the best static policy was selected independently from the constant-operation grid. However, none of these static baseline policies satisfied the main conversion feasibility threshold. The static baseline is therefore interpreted as an unconstrained constant-operation benchmark rather than a feasible operating strategy under the main constraint definition. Relative to this benchmark, the dynamic Pareto policies improved ethanol titer by 10.6%, productivity by 8.3%, and substrate conversion by 14.3%. These results indicate that dynamic temperature and pH scheduling offers a measurable advantage over constant-condition operation for the main performance-oriented objectives when feasibility is taken into account (Table 4).

The ethanol–productivity comparison provides further evidence of this advantage. The static constant-operation baselines occupy a lower productivity–titer region, whereas the dynamic policy archive extends toward higher ethanol and productivity values. The feasible dynamic Pareto policies define the upper performance envelope in this objective space, indicating that the dynamic search identifies operating policies that outperform the constant-operation alternatives for the primary process-performance objectives (Figure 2).

Table 4. Comparison between dynamic Pareto policies and the best static constant-operation baselines. Static baselines were selected independently for each criterion from the constant-temperature/constant-pH grid. None of the selected static baselines satisfied the main conversion feasibility threshold.

Criterion	Dynamic value	Static baseline	Improvement (%)	T_{static} (°C)	pH_{static} (-)	t_f (h)
Max ethanol titer	1.265	1.144	10.6	48.0	5.5	144.0
Max productivity	0.0170	0.0157	8.3	48.0	5.5	63.0
Max conversion	0.440	0.384	14.3	49.0	5.4	144.0

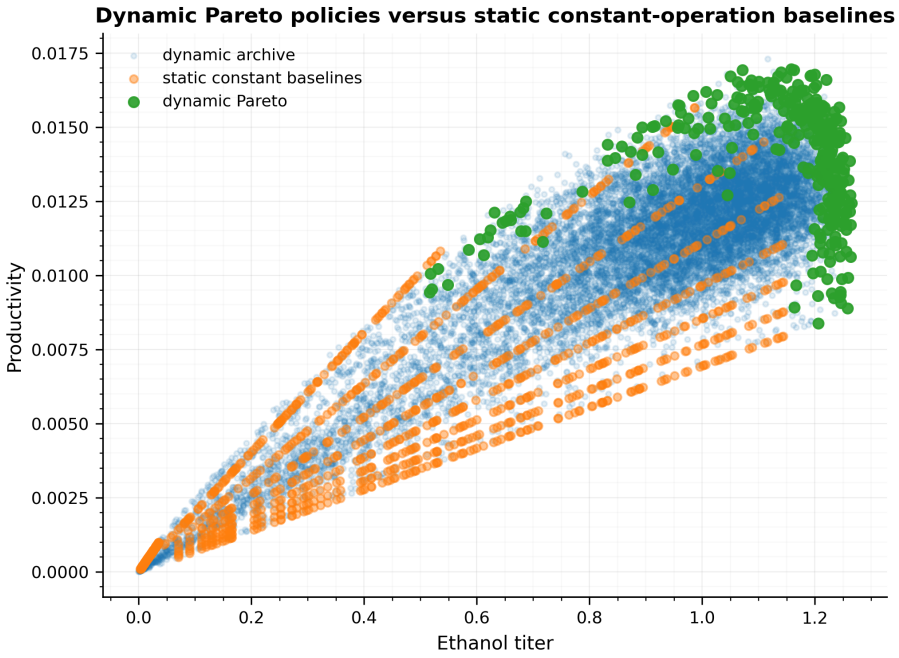

Figure 2. Comparison of dynamic policy candidates, static constant-operation baselines, and feasible dynamic Pareto policies in ethanol–productivity objective space.

 doi:10.20944/preprints202605.0590.v1

4.2. Many-Objective Pareto Structure

The many-objective structure of the feasible Pareto set is summarized in Table 5. The final feasible Pareto set contained 328 non-dominated policies satisfying the primary feasibility criterion $X_{conv} \geq 0.42$. Across this set, the policies spanned distinct ranges in ethanol titer, productivity, substrate conversion, sugar accumulation, operating severity, control movement, and batch duration. This spread indicates that no single operating policy can simultaneously optimize all objectives. Instead, improvement in one performance dimension is generally accompanied by deterioration in at least one other.

In particular, policies that favor high ethanol titer and high substrate conversion tend to require longer batch durations or higher average sugar accumulation, whereas policies that prioritize shorter batch times, lower operating severity, or lower control movement sacrifice some titer or conversion performance. The many-objective summary therefore reinforces the central conclusion of the study: CBP operation is characterized by a structured set of trade-offs rather than by a single universally optimal operating point. This interpretation is consistent with the role of Pareto analysis in multi-objective process optimization, where the main value lies in revealing decision-relevant compromises rather than collapsing them into a single scalar optimum [10,12].

Table 5. Objective-space summary of the feasible Pareto-optimal CBP policies at $X_{conv} \geq 0.42$. For ethanol titer, productivity, and conversion, higher values are preferred; for average sugar, operating severity, control movement, and batch time, lower values are preferred.

Objective	Best Pareto value	Median Pareto value	Worst Pareto value
Ethanol titer (g L^{-1})	1.265	1.203	0.517
Productivity (g L^{-1} h^{-1})	0.01696	0.01418	0.00838
Substrate conversion (-)	0.4395	0.428	0.420
Average sugar (g L^{-1})	0.236	0.427	0.578
Operating severity (-)	0.027	0.052	0.140
Control movement (-)	0.0038	0.0230	0.1436
Batch time (h)	51.5	80.4	143.9

4.3. Distribution of the Evaluated Policy Archive

Before extracting the feasible Pareto set, the full evaluated archive was examined to assess the breadth of the dynamic policy search. The archive-level distributions show that the search was not confined to a narrow operating region, but instead sampled a broad range of ethanol titers, productivities, substrate conversions, and batch durations. Final ethanol and productivity distributions were concentrated toward the upper-performing region, whereas conversion values approached the imposed feasibility boundary. The batch-time distribution was centered around intermediate operating durations, with additional exploration of shorter high-productivity policies and longer high-conversion policies. This archive-level perspective supports the subsequent Pareto analysis by showing that the non-dominated set was extracted from a broad population of candidate dynamic policies rather than from a narrowly constrained local search [10,12] (Figure 3).

 doi:10.20944/preprints202605.0590.v1

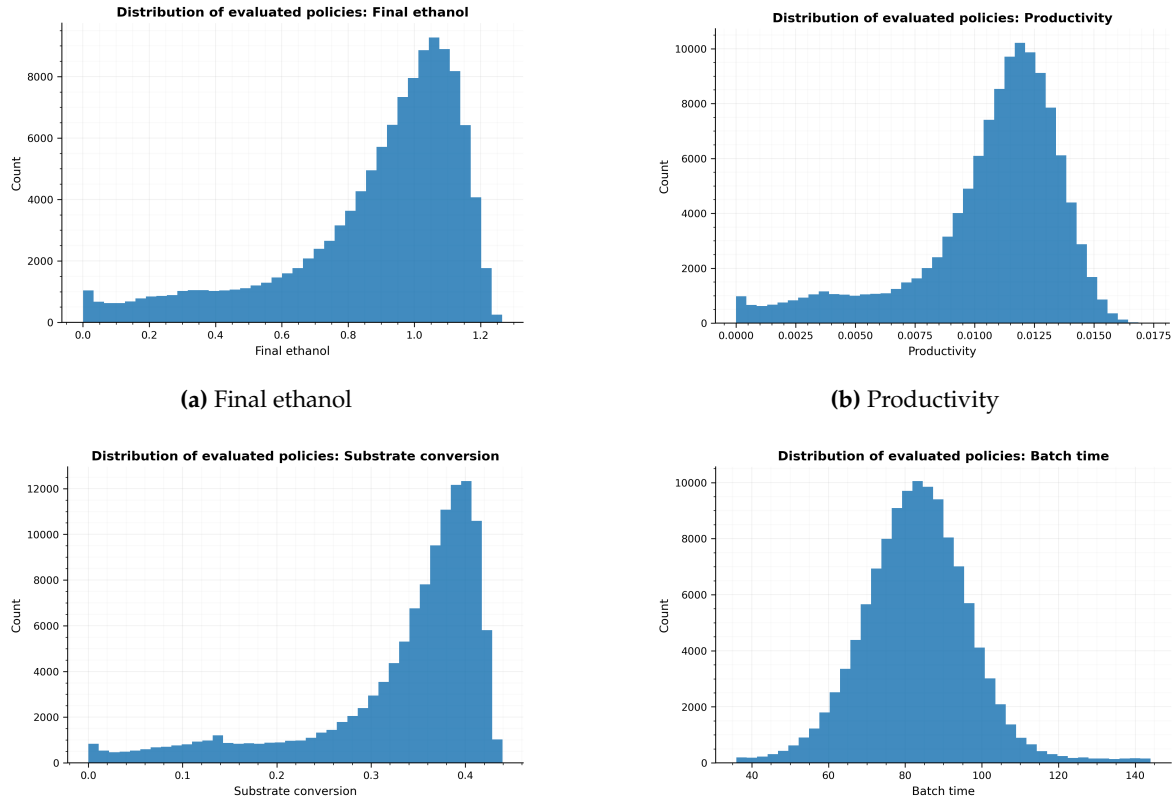

(a) Final ethanol **(b)** Productivity

(c) Substrate conversion **(d)** Batch time

Figure 3. Distributions of key performance metrics across the evaluated dynamic-policy archive. These histograms summarize the full candidate population before feasible Pareto filtering.

4.4. Representative Pareto-Optimal Policies

To improve the interpretability of the feasible Pareto set, a small set of representative policies was extracted to reflect different process priorities. The maximum-ethanol policy achieved 1.265 g L^{-1} ethanol at a batch time of 101.7 h, whereas the maximum-productivity policy reduced the batch time to 68.3 h and achieved 0.0170 g L^{-1} h^{-1}. The maximum-conversion policy reached a substrate conversion of 0.440 while still producing 1.214 g L^{-1} ethanol. In contrast, the balanced-knee policy provided a compromise solution, combining 1.216 g L^{-1} ethanol, 0.0145 g L^{-1} h^{-1} productivity, and 0.434 conversion at 83.8 h.

These representative policies demonstrate that different operating priorities lead to distinct compromises among ethanol titer, productivity, conversion, sugar accumulation, operating severity, and batch duration. In particular, a policy that strongly favors one objective does not necessarily remain attractive once the other objectives are considered simultaneously. The balanced-knee policy is therefore useful as an interpretable compromise solution, whereas the extreme policies help define the practical limits of the feasible Pareto set. The representative-policy summary is provided in Table 6.

Table 6. Representative feasible Pareto-optimal dynamic CBP policies.

Policy	Ethanol (g L^{-1})	Prod. (g L^{-1} h^{-1})	Conv. (-)	Avg. sugar (g L^{-1})	Severity (-)	Movement (-)	Time (h)
Max ethanol	1.265	0.0124	0.427	0.353	0.044	0.022	101.7
Max productivity	1.158	0.0170	0.430	0.473	0.054	0.030	68.3
Max conversion	1.214	0.0132	0.440	0.431	0.076	0.047	91.8
Min sugar	1.206	0.0084	0.420	0.236	0.052	0.030	143.9
Min severity	1.255	0.0121	0.420	0.325	0.027	0.016	104.0
Min batch time	0.518	0.0101	0.427	0.544	0.075	0.015	51.5
Balanced knee	1.216	0.0145	0.434	0.416	0.046	0.023	83.8

 doi:10.20944/preprints202605.0590.v1

4.5. Pairwise Pareto Trade-Offs

The pairwise trade-off plots provide further insight into the structure of the feasible CBP operating region. The ethanol–productivity relationship is favorable across much of the feasible set, but the policies with the highest ethanol titers do not always coincide with those having the highest productivities, because higher final ethanol concentrations are often obtained only at longer batch durations. This trade-off between terminal performance and time-normalized performance is typical in dynamic bioprocess optimization [10].

The ethanol–severity plot indicates that relatively high ethanol titers can still be achieved at moderate operating severity, suggesting that strongly aggressive temperature and pH scheduling is not always required to approach the upper ethanol region. The conversion–batch-time trade-off shows that policies with higher substrate conversion generally require longer residence times, and that many feasible Pareto points cluster near the upper conversion boundary. This behavior is consistent with earlier Pareto analyses of bioreactor operation, where improvement in one performance target often requires accepting deterioration in another [23].

The sugar–ethanol relationship shows that higher ethanol production is generally associated with moderate soluble-sugar accumulation during the hydrolysis-dominant portion of the batch, although the representative Pareto policies remain below the imposed soft sugar limit. Overall, these trade-offs confirm that CBP operation does not admit a single universal optimum. Instead, the preferred operating policy depends on how decision makers prioritize ethanol titer, productivity, conversion, operating severity, and batch duration. This is precisely the setting in which Pareto-based multi-objective optimization provides the greatest insight [12]. The corresponding pairwise Pareto relationships are shown in Figure 4.

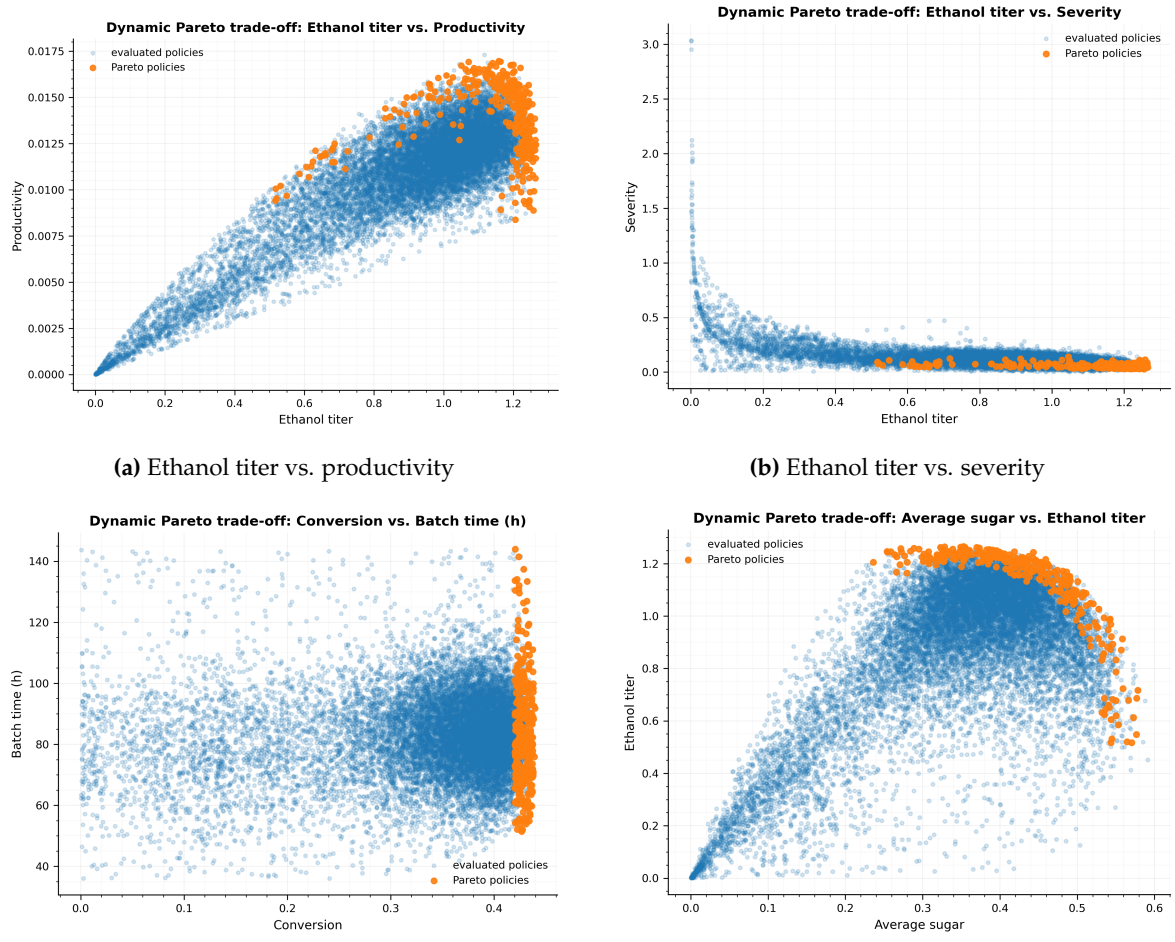

(a) Ethanol titer vs. productivity

(b) Ethanol titer vs. severity

(c) Conversion vs. batch time

(d) Average sugar vs. ethanol titer

Figure 4. Pairwise Pareto trade-offs for feasible dynamic CBP operating policies.

 doi:10.20944/preprints202605.0590.v1

4.6. Dynamic Operating-Policy Maps

Representative temperature and pH profiles are presented in Figure 5. Most high-performing policies operate within a narrow range, roughly 47–50 °C and pH 5.2–5.9. This indicates that strong CBP performance does not require highly erratic control behavior. Instead, it is associated with deliberate time-dependent adjustments within a biologically favorable operating window.

Clear distinctions are nevertheless visible among the different policy groups. The high-ethanol and high-conversion policies tend to maintain moderately elevated temperatures during the hydrolysis-dominant part of the batch before shifting toward milder conditions near the end of the process. By contrast, the minimum-severity and balanced-knee policies show smoother behavior and remain closer to the nominal preferred region throughout most of the batch. These differences illustrate how alternative CBP decision priorities are translated into distinct dynamic operating trajectories (Figure 5).

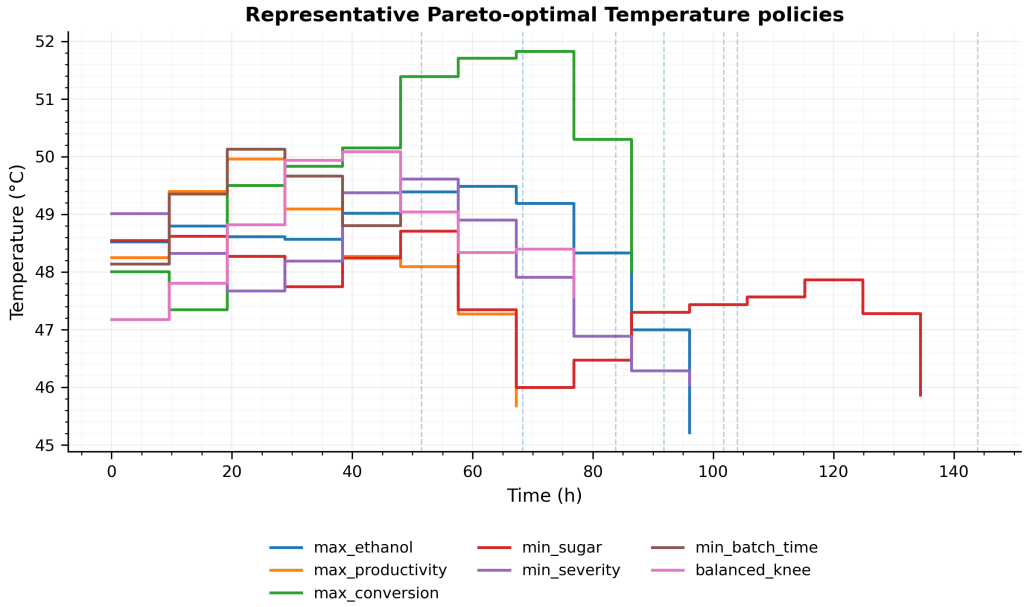

(a) Temperature policies

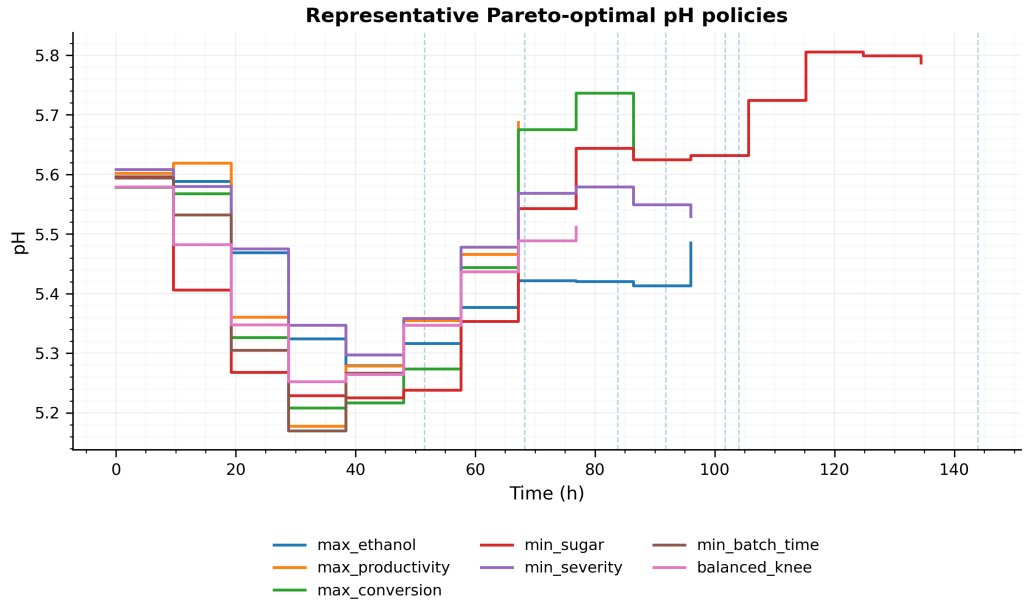

(b) pH policies

Figure 5. Representative dynamic temperature and pH policies selected from the Pareto set.

 doi:10.20944/preprints202605.0590.v1

The policy maps in Figure 6 provide a compact comparison of these operating strategies across the full time grid. These visualizations are especially useful because they directly connect decision priorities, such as high ethanol titer, high conversion, or low severity, with the corresponding time-dependent operating choices. In this way, the Pareto analysis goes beyond objective-value reporting and provides practical guidance on how the reactor can be operated under different performance priorities (Figure 6).

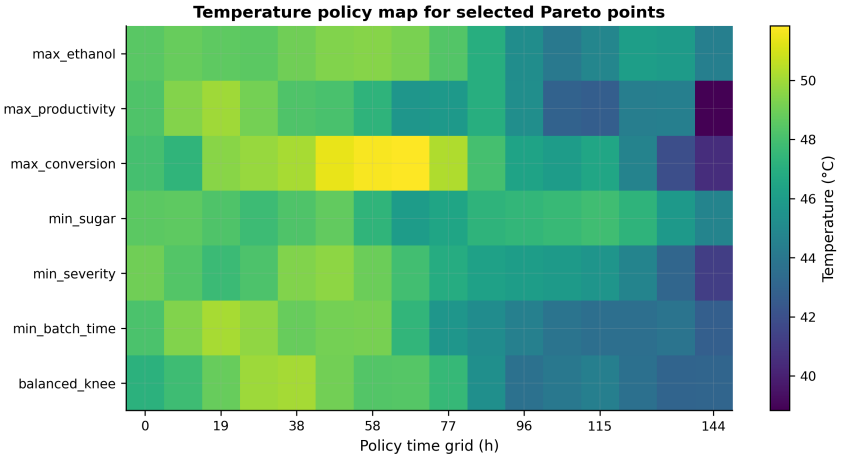

(a) Temperature policy map

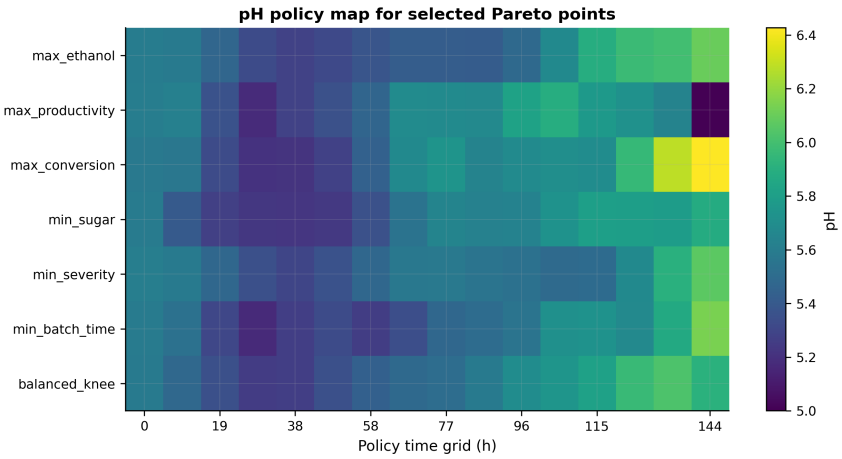

(b) pH policy map

Figure 6. Operating-policy maps for representative Pareto-optimal CBP policies.

4.7. State Trajectories Under Representative Pareto Policies

The representative state trajectories provide additional insight into how the selected Pareto policies balance hydrolysis and fermentation over time. Ethanol production begins after the early hydrolysis-dominant stage and reaches approximately 1.2–1.27 g L^{-1} for most of the higher-performing policies. At the same time, soluble sugar accumulates during the middle part of the batch and then declines as fermentation becomes more dominant. This behavior is consistent with the intended CBP process dynamics, where hydrolysis first builds the soluble-sugar pool and fermentation subsequently consumes it to produce ethanol.

All representative trajectories remain below the imposed soft sugar constraint, confirming that the Pareto policies avoid excessive sugar buildup while still sustaining ethanol production. The insoluble-substrate trajectories further show that most substrate conversion occurs during the middle part of the batch. After this stage, substrate depletion slows and additional residence time gives diminishing returns. This helps explain why some long-batch policies provide only modest additional gains in conversion or ethanol relative to shorter balanced policies (Figure 7).

 doi:10.20944/preprints202605.0590.v1

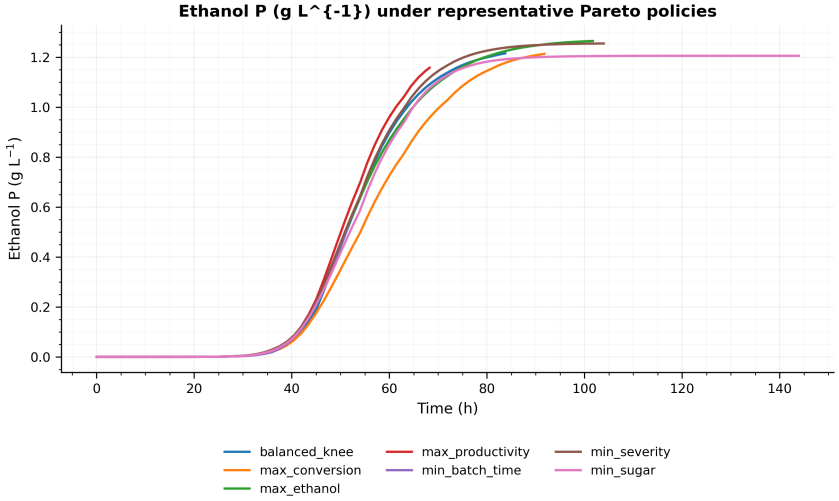

(a) Ethanol

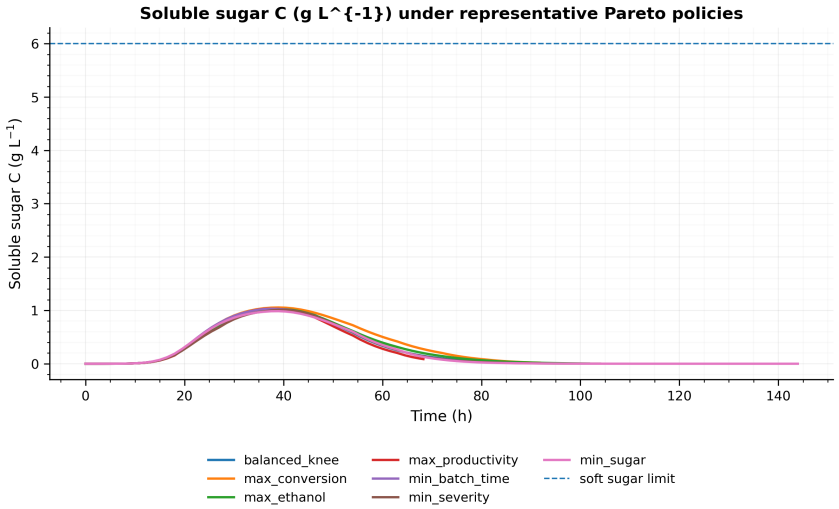

(b) Soluble sugar

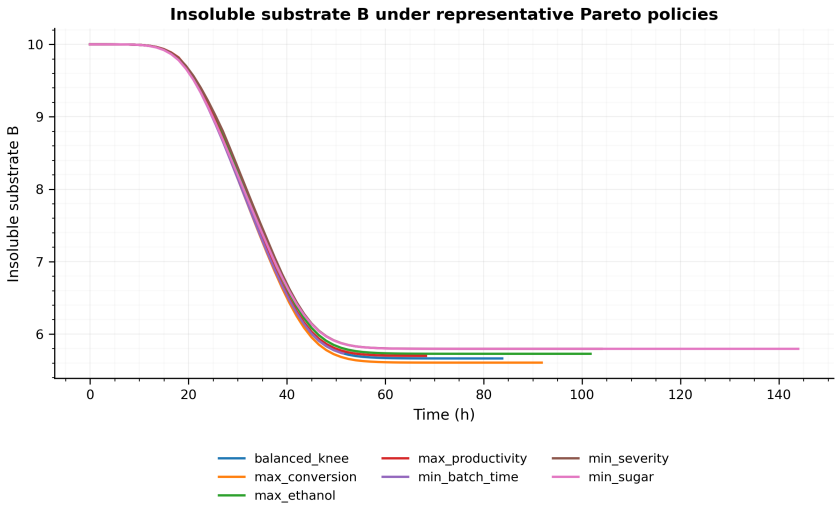

(c) Insoluble substrate

Figure 7. Dynamic state trajectories for representative feasible Pareto-optimal policies, showing ethanol formation, soluble-sugar accumulation and consumption, and insoluble-substrate depletion over the batch horizon.

 doi:10.20944/preprints202605.0590.v1

4.8. Feasibility-Threshold Sensitivity and Independent-Seed Repeatability

The selected feasibility threshold strongly affected the number of policies classified as feasible, but it did not change the maximum attainable ethanol titer over the tested range. At minimum conversion thresholds of 0.35, 0.38, and 0.40, large feasible policy sets were obtained. At the main threshold of 0.42, 5,017 feasible policies remained, corresponding to 4.18% of the evaluated archive. No feasible policies were found at thresholds of 0.44 or 0.55. These results indicate that 0.42 is a strict but attainable feasibility cutoff for the current model, whereas 0.44 and 0.55 fall outside the attainable conversion region under the present operating bounds and model assumptions (Table 7).

Because the Pareto search relies on randomized policy initialization and stochastic evolutionary refinement, independent-seed repeatability was also evaluated. Three additional reduced-budget optimization runs were performed using the same model, constraints, and operating bounds. The maximum ethanol titer remained within a narrow range of 1.2624–1.2637 g L^{-1}, while the maximum conversion remained between 0.4375 and 0.4386. Although the number of feasible and non-dominated policies varied across seeds, the attainable high-performance region remained stable. This supports the conclusion that the main Pareto structure is not an artifact of a single random initialization, but rather a robust feature of the dynamic search space under the present formulation (Table 8 and Figure 8).

Table 7. Sensitivity of feasible policy counts to the minimum conversion threshold.

Min. conversion threshold	Feasible policies	Feasible fraction	Max ethanol (g L^{-1})	Max conversion (-)
0.35	70,651	0.589	1.265	0.4395
0.38	46,343	0.386	1.265	0.4395
0.40	24,620	0.205	1.265	0.4395
0.42	5,017	0.0418	1.265	0.4395
0.44	0	0.000	–	–
0.55	0	0.000	–	–

Table 8. Independent-seed repeatability of the dynamic Pareto optimization.

Seed	Evaluated policies	Feasible policies	Pareto policies	Max ethanol (g L^{-1})	Max conversion (-)
1042	19,000	698	212	1.2627	0.4386
2042	19,000	165	92	1.2637	0.4379
3042	19,000	728	221	1.2624	0.4375

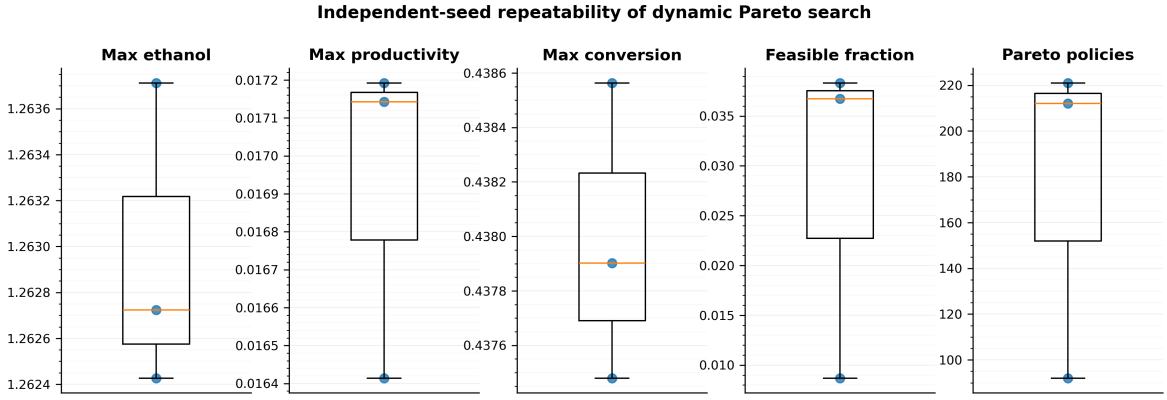

Figure 8. Independent-seed repeatability of the dynamic Pareto search. The repeated runs show that the high-performance region is stable across random initializations, although the number of feasible and non-dominated policies varies with the stochastic search path.

 doi:10.20944/preprints202605.0590.v1

4.9. Interpretation of Results and Value for Bioprocess Optimization and Control

The Pareto results reveal coupled trade-offs among key process variables in CBP operation. Ethanol titer, productivity, and substrate conversion are positively correlated over much of the feasible space, but they favor different batch durations and operating policies. High-titer and high-conversion policies generally require longer batches, whereas high-productivity policies favor earlier termination. Similar behavior has been observed in multi-objective optimization of fed-batch and other bioprocess systems, where yield, titer, productivity, operating time, and cost cannot usually be optimized simultaneously because of competing process requirements [10,23]. For bioethanol production, multi-objective formulations have also shown that time-dependent operation can reveal trade-offs that remain hidden in single-objective analysis [24]. In the present CBP model, low-severity operation remains feasible, but careful dynamic temperature and pH scheduling is required to preserve ethanol performance.

The static baseline analysis further shows that constant-temperature and constant-pH policies cannot satisfy the main feasibility threshold in this model. Dynamic operation is therefore important not only for improving ethanol titer and productivity, but also for reaching the stricter conversion target. This supports the use of dynamic optimization rather than fixed-condition screening for CBP operation. Similar arguments have been made in fermentation and biorefinery optimization studies, where time-dependent operating policies can reveal performance improvements and feasibility constraints that are overlooked in static or single-objective formulations [24,25]. More broadly, model-driven fermentation studies emphasize that dynamic models can support scale-up, process monitoring, and operational decision making when used within a suitable optimization or control framework [5].

These results complement recent modeling and machine-learning studies of CBP processes. Previous work has shown that CBP datasets and predictive models can support endpoint-level analysis of ethanol and co-product formation [8,9]. Other CBP modeling studies have emphasized the need for mechanistic understanding of substrate conversion, microbial behavior, and process limitations [15]. The focus here is different: rather than predicting endpoint performance alone, the Pareto framework maps the within-batch operating landscape and links process priorities directly to dynamic temperature and pH schedules.

The feasibility-threshold analysis provides an additional layer of decision support. A conversion threshold of 0.42 is strict but attainable, whereas thresholds of 0.44 and 0.55 are not attainable under the present model and operating bounds. This distinction is important because treating an infeasible target as a normal operating requirement can lead to misleading process conclusions. In this sense, the Pareto framework acts not only as an optimizer, but also as a diagnostic tool for identifying realistic performance limits and feasible compromise regions. Pareto-based decision support is widely used in multi-objective process optimization because it allows process engineers to select policies according to explicit priorities rather than relying on a single arbitrarily weighted scalar objective [12,13]. Normalized normal constraint and related methods further illustrate how structured Pareto-front generation can support decision making when objectives conflict [14,26].

The results also clarify how the present approach differs from batch-to-batch learning. The objective is not to update operating policies across repeated batches using endpoint data, but to characterize the within-batch dynamic operating landscape through Pareto optimization. The resulting fronts, policy maps, and representative trajectories provide interpretable guidance for selecting operating strategies according to priorities such as high ethanol titer, short batch duration, low severity, or balanced operation. This makes the approach complementary to adaptive learning and model predictive control methods: offline Pareto maps can identify promising operating regions, while future online controllers can adjust selected policies as measurements become available during the batch [10,11,27].

4.10. Limitations and Future Directions

The findings should be interpreted as model-based optimization outcomes. The kinetic model uses lumped substrate, sugar, biomass, enzyme, and ethanol states, and the resulting Pareto policies depend on the assumed parameterization of temperature and pH effects. This reduced-order

 doi:10.20944/preprints202605.0590.v1

structure enables large-scale dynamic policy search, but it does not resolve feedstock heterogeneity, detailed cellulose depolymerization, intracellular metabolism, microbial community dynamics, or competing fermentation products. More detailed CBP models, including genome-scale, cybernetic, and population-balance formulations, could be used in future work to test whether the same Pareto trade-offs persist under higher-fidelity biological representations [6,7,15].

The present study is deterministic and does not include parameter uncertainty, experimental measurement noise, contamination risk, or unmodeled feedstock variability. The feasibility threshold is also model-dependent. The sensitivity analysis indicates that conversion targets above 0.44 are not attainable under the current operating bounds, but this limit may shift if the kinetic parameters, substrate representation, pretreatment assumptions, or reactor configuration are revised. Future studies should therefore extend the formulation to robust or uncertainty-aware Pareto optimization. Robust multi-objective optimal control and dynamic optimization under uncertainty provide useful methodological foundations for this extension [19,20]. Multi-objective optimal experimental design could also be used to select experiments that improve parameter identifiability while testing informative regions of the Pareto front [11].

Future work should also validate selected representative policies experimentally. A practical next step would be to test a small subset of Pareto policies, such as the maximum-ethanol, maximum-productivity, minimum-severity, and balanced-knee policies, in controlled batch experiments. The resulting data could be used to recalibrate the kinetic model and update the Pareto front. Literature-derived endpoint datasets could also be connected with dynamic optimization by using broader CBP data resources to inform parameter priors, feasible operating ranges, and experimental policy selection [9]. Finally, the offline Pareto policies developed here could be incorporated into model predictive control, allowing temperature and pH trajectories to be adjusted online as sugar and ethanol measurements become available during CBP operation [5,10,27].

5. Summary and Conclusions

The current study formulates CBP as a multi-objective dynamic optimization problem incorporating feasibility considerations. Instead of optimizing ethanol titer at the conclusion of the batch, the problem formulation includes titer, productivity, substrate conversion, total accumulation of soluble sugars, operating severity, control movement, and batch time. Policies for time-variation of temperature and pH in combination with terminal batch time were optimized to produce feasible Pareto-optimal CBP strategies.

The primary optimization examined 120,000 dynamic policies of which 5,017 satisfied the key feasibility requirement and 328 were found to be feasible Pareto-optimal policies. For the former, the best dynamic policy resulted in a titer of 1.265 g L^{-1}; the best productivity reached 0.017 g L^{-1} h^{-1}, and the highest substrate conversion was 0.440. Compared to the best static constant-operation baseline, dynamic Pareto policies improve ethanol titer by 10.6%, productivity by 8.3%, and substrate conversion by 14.3%. The above result demonstrates the benefits achievable with dynamic scheduling of temperature and pH relative to constant-operation.

The Pareto-optimal outcomes support the notion that CBP operation involves structured trade-offs as opposed to one universal optimum. High titer and conversion policies typically resulted in long batch duration, whereas high productivity and short batch policies tolerated lower final ethanol concentration. In addition, the feasibility-threshold analysis revealed that a conversion threshold of 0.42 is realistic and attainable but the thresholds of 0.44 and 0.55 are unrealistic and unattainable within the considered bounds. Lastly, independent-seed runs confirmed that the best values of ethanol titer and substrate conversion are repeatable across stochastic optimization runs.

In summary, the current work introduces a framework for generating and evaluating interpretable dynamic CBP policies as a decision-support tool for CBP design. The results are based on a model of the process rather than experimental measurements. Thus, future research should consider robust

 doi:10.20944/preprints202605.0590.v1

Pareto optimization under uncertainty, integration of economic and life-cycle considerations, and experimental testing of optimal policies.

Supplementary Materials: The following supporting information can be downloaded at the website of this paper posted on Preprints.org.

Author Contributions: Conceptualization, M.K.Y.; methodology, M.K.Y.; validation, M.K.Y. and A.A.; formal analysis, M.K.Y.; investigation, M.K.Y. and N.Y.A.; data curation, M.K.Y.; visualization, M.K.Y.; writing—original draft preparation, M.K.Y.; writing—review and editing, N.Y.A. and A.A.; supervision, N.Y.A. and A.A. All authors have read and agreed to the published version of the manuscript.

Funding: This work was partly supported by the German Academic Exchange Service (DAAD) under the programme Research Grants – Bi-nationally Supervised Doctoral Degrees/Cotutelle (Grant No. 57693451).

Institutional Review Board Statement: Not applicable.

Informed Consent Statement: Not applicable.

Data Availability Statement: The original contributions presented in this study are included in the article. Further inquiries can be directed to the corresponding author.

Acknowledgments: The authors acknowledge support from the Open Access Publication Fund of the University of Duisburg-Essen, the German Academic Exchange Service (DAAD), and the KNUST Engineering Education Project (KEEP).

Conflicts of Interest: The authors declare no conflict of interest.

References

1. Lynd, L.R.; Weimer, P.J.; van Zyl, W.H.; Pretorius, I.S. Microbial cellulose utilization: Fundamentals and biotechnology. *Microbiology and Molecular Biology Reviews* **2002**, *66*, 506–577. https://doi.org/10.1128/MMBR.66.3.506-577.2002.
2. Lynd, L.R.; van Zyl, W.H.; McBride, J.E.; Laser, M. Consolidated bioprocessing of cellulosic biomass: An update. *Current Opinion in Biotechnology* **2005**, *16*, 577–583. https://doi.org/10.1016/j.copbio.2005.08.009.
3. Akinosho, H.; Yee, K.; Close, D.; Ragauskas, A. The emergence of Clostridium thermocellum as a high utility candidate for consolidated bioprocessing applications. *Frontiers in Chemistry* **2014**, *2*, 66. https://doi.org/10.3389/fchem.2014.00066.
4. Salehi Jouzani, G.; Taherzadeh, M.J. Advances in consolidated bioprocessing systems for bioethanol and butanol production from biomass: A comprehensive review. *Biofuel Research Journal* **2015**.
5. Du, Y.H.; Wang, M.Y.; Yang, L.H.; Tong, L.L.; Guo, D.S.; Ji, X.J. Optimization and scale-up of fermentation processes driven by models. *Bioengineering* **2022**, *9*, 473. https://doi.org/10.3390/bioengineering9090473.
6. Garcia, S.; Thompson, R.A.; Giannone, R.J.; et al. Development of a genome-scale metabolic model of Clostridium thermocellum and its applications for integration of multi-omics datasets and computational strain design. *Frontiers in Bioengineering and Biotechnology* **2020**, *8*, 772. https://doi.org/10.3389/fbioe.2020.00772.
7. Ahamed, F.; Song, H.S.; Ho, Y.K. Modeling coordinated enzymatic control of saccharification and fermentation by Clostridium thermocellum during consolidated bioprocessing of cellulose. *Biotechnology and Bioengineering* **2021**. https://doi.org/10.1002/bit.27705.
8. Yeboah, M.K.; Asiedu, N.Y.; Dogbe, S.; Addo, A. Performance of Machine Learning Based-Modelling Approach in Consolidated Bioprocessing with Microbial Consortium for Bioethanol Production. *Industrial Biotechnology* **2024**, *20*, 77–97.
9. Yeboah, M.K.; Addo, A.; Asiedu, N.Y. Multi-Product Modeling of Consolidated Bioprocessing Using a Literature-Derived Dataset: A Multi-Output Learning Framework for Ethanol and Co-Products. *Fermentation* **2026**, *12*, 224. https://doi.org/10.3390/fermentation12050224.
10. Logist, F.; Telen, D.; Houska, B.; Diehl, M.; Van Impe, J.F. Multi-objective optimal control of dynamic bioprocesses using ACADO Toolkit. *Bioprocess and Biosystems Engineering* **2013**, *36*, 555–569. https://doi.org/10.1007/s00449-012-0770-9.

 doi:10.20944/preprints202605.0590.v1

11. Telen, D.; Logist, F.; Van Derlinden, E.; Tack, I.; Van Impe, J.F. Optimal experiment design for dynamic bioprocesses: A multi-objective approach. *Chemical Engineering Science* **2012**, *78*, 82–97. https://doi.org/10.1016/j.ces.2012.04.052.
12. Deb, K.; Pratap, A.; Agarwal, S.; Meyarivan, T. A fast and elitist multiobjective genetic algorithm: NSGA-II. *IEEE Transactions on Evolutionary Computation* **2002**, *6*, 182–197. https://doi.org/10.1109/4235.996017.
13. Das, I.; Dennis, J.E. Normal-boundary intersection: A new method for generating the Pareto surface in nonlinear multicriteria optimization problems. *SIAM Journal on Optimization* **1998**, *8*, 631–657. https://doi.org/10.1137/S1052623496307510.
14. Messac, A.; Ismail-Yahaya, A.; Mattson, C.A. The normalized normal constraint method for generating the Pareto frontier. *Structural and Multidisciplinary Optimization* **2003**, *25*, 86–98. https://doi.org/10.1007/s00158-002-0276-1.
15. Yeboah, M.K.; Söffker, D. Consolidated Bioprocessing of Lignocellulosic Biomass: A Review of Experimental Advances and Modeling Approaches. *Bioresources and Bioproducts* **2026**, *2*. https://doi.org/10.3390/bioresourbioprod2010004.
16. Linville, J.L.; Rodriguez, M.; Mielenz, J.R.; Cox, C.D. Kinetic modeling of batch fermentation for Populus hydrolysate tolerant mutant and wild type strains of Clostridium thermocellum. *Bioresource Technology* **2013**, *147*, 605–613. https://doi.org/10.1016/j.biortech.2013.08.112.
17. Dash, S.; Khodayari, A.; Zhou, J.; Holwerda, E.K.; Olson, D.G.; Lynd, L.R.; Maranas, C.D. Development of a core Clostridium thermocellum kinetic metabolic model consistent with multiple genetic perturbations. *Biotechnology for Biofuels* **2017**, *10*, 108. https://doi.org/10.1186/s13068-017-0792-2.
18. Wang, F.S.; Yang, M.Y.; Chen, M.L. Optimal temperature and pH control for a batch simultaneous saccharification and co-fermentation process. *Chemical Engineering Communications* **2015**, *202*, 1083–1095. https://doi.org/10.1080/00986445.2014.886200.
19. Logist, F.; Houska, B.; Diehl, M.; Van Impe, J.F. Robust multi-objective optimal control of uncertain (bio)chemical processes. *Chemical Engineering Science* **2011**, *66*, 4670–4682. https://doi.org/10.1016/j.ces.2011.06.017.
20. Nimmegeers, P.; Telen, D.; Logist, F.; Van Impe, J.F. Dynamic optimization of biological networks under parametric uncertainty. *BMC Systems Biology* **2016**, *10*. https://doi.org/10.1186/s12918-016-0328-6.
21. Taras, S.; Woinaroschy, A. An interactive multi-objective optimization framework for sustainable design of bioprocesses. *Computers & Chemical Engineering* **2012**.
22. Miettinen, K. *Nonlinear Multiobjective Optimization*; Kluwer Academic Publishers: Boston, 1999. https://doi.org/10.1007/978-1-4615-5563-6.
23. Sarkar, D.; Modak, J.M. Pareto-optimal solutions for multi-objective optimization of fed-batch bioreactors using nondominated sorting genetic algorithm. *Chemical Engineering Science* **2005**, *60*, 481–492. https://doi.org/10.1016/j.ces.2004.07.130.
24. Darkwah, K.; Knutson, B.L.; Seay, J.R. Multi-objective versus single-objective optimization of batch bioethanol production based on a time-dependent fermentation model. *Clean Technologies and Environmental Policy* **2018**, *20*, 1821–1832. https://doi.org/10.1007/s10098-018-1553-z.
25. Flevaris, K.; Chatzidoukas, C. Optimal fed-batch bioreactor operating strategies for the microbial production of lignocellulosic bioethanol and exploration of their economic implications: A step forward towards commercial second-generation bioethanol. *Journal of Cleaner Production* **2021**, *295*, 126384. https://doi.org/10.1016/j.jclepro.2021.126384.
26. Ögmundarson, Ó.; Sukumara, S.; Herrgård, M.J.; Fantke, P. Combining environmental and economic performance for bioprocess optimization. *Trends in Biotechnology* **2020**, *38*, 1203–1214. https://doi.org/10.1016/j.tibtech.2020.04.011.
27. Rajasekhar, N.; Radhakrishnan, T.K.; Mohamed, S.N. Reinforcement learning based temperature control of a fermentation bioreactor for ethanol production. *Biotechnology and Bioengineering* **2024**. https://doi.org/10.1002/bit.28784.